

1 Presented at DIS2022: XXIX International Workshop on Deep-Inelastic Scattering and Related Sub-
2 jects, Santiago de Compostela, Spain, May 2-6 2022.

3 **Probing hadronization and jet substructure with leading particles in jet at H1**

4 Mriganka Mouli Mondal ¹

5 CFNS, Stony Brook University

6 **Abstract**

7 We measure the charge and momentum correlations (r_c) of the two leading momentum parti-
8 cles in a jet. The observable, r_c used is expected to be very sensitive to fragmentation dynamics.
9 The measurement is made with various kinematic variables and in particular the formation time
10 (t_{form}) brings the information of when the di-hadron fragmentation occurred separating the regions
11 dominated by perturbative or non-perturbative dynamics. The associated structure in jet in terms
12 of partonic branching is studied via jet substructure and recursive soft drop using recursive soft
13 drop technique. An association of subjects to the leading particles and the related correlations is
14 framed to extract r_c which is more resembles as partonic branching. It is revealing that soft and
15 core part of the fragmentation significantly differ in building r_c correlations in large formation
16 time region.

17 **1 Introduction: Observable**

In the process of fragmentation the two-particle correlation of the leading charged hadron h_1 and
next-to-leading charged hadron h_2 is studied with charge correlations [1, 2]. The charge correlation
ratio, r_c , is defined from the differential cross sections $d\sigma_{h_1 h_2}/dX$ to quantify flavor and kinematic
dependence of hadronization in the production of h_1 and h_2 or \bar{h}_2 (the anti-particle of h_2),

$$r_c(X) = \frac{d\sigma_{h_1 h_2}/dX - d\sigma_{h_1 \bar{h}_2}/dX}{d\sigma_{h_1 h_2}/dX + d\sigma_{h_1 \bar{h}_2}/dX}. \quad (1)$$

18 We will explore the dependence of r_c on a variety of kinematic variables, X . In the definition, Eq. (1),
19 h_1 and h_2 can in principle be arbitrary hadron species, including charged and neutral hadrons. We
20 will select the events only in the case where both of them are charged particles. The r_c is negative
21 for the cases where $h_1 \bar{h}_2$ cases dominate over $h_1 h_2$ and in the string breaking picture opposite pair
22 production dominates that leads to r_c value be between 0 and -1 .

23
24 Formation time, $t_{\text{form}} = \frac{[2z(1-z)P]}{k_{\perp}^2}$, is calculated from leading (h_1) and next-to-leading (h_2) hadron's
25 kinematics. Leading and next-to-leading hadrons in jets are selected in terms of the momentum
26 fraction along the jet axis. In formulating the formation time, z and P are defined as follows $z =$
27 $P_{h_2}/(P_{h_2} + P_{h_1})$, $P_{h_1} = (1 - z)P$ and $P_{h_2} = zP$. Formation time can be related to time scale of
28 hadronization where Small formation time corresponds small z or large k_{\perp} . For a specific z (specific
29 P_{h_2} and P_{h_1} magnitudes), a large θ or large k_{\perp} corresponds to a small t_{form} resulting in early de-
30 correlations and the region is dominated by wide angle gluon radiations. On the contrary a small θ
31 corresponds to small k_{\perp} and this is the region for large t_{form} .

32 Building r_c correlations with partonic branches is made with angular ordered clusters and this fits
33 with the picture where the struck parton undergoes perturbative shower evolution. The charges of a
34 prong is assigned as the charge of the leading particle within.

¹(for the H1 Collaboration) [H1prelim-22-032]

2 Data and MC samples and event selection

The data were taken by the H1 experiment during 2003-2007 using 27.6 GeV electron/positron scatterers off 920 GeV proton at HERA, which corresponds to a center-of-mass energy $\sqrt{s} = 319$ GeV. The data are selected requiring functional central trackers (CJC1, CJC2) and calorimeters (LAr, SpaCal). The MC samples are reconstructed using the same detector condition of the corresponding years with Djangoh 1.4 and Rappag 3.1 event generator. Subtrigger ST67 is used and it is sufficient for our interest in getting relatively high Q^2 (> 150 GeV²) events and with good tracking using central detectors. The z -vertex distribution spreads widely mostly due to the 107 colliding bunch size in the accelerator while the transverse spread is narrow. The interaction region in the z direction in this analysis is required to be less than ± 30 cm. The longitudinal momentum of Hadronic Final State (HFS) and the scattered electron ($E - p_z$) is expected to be two times the incident electron energy, i.e., 55.2 GeV. The spread in the variable ($E - p_z$) appears due to experimental resolution effects in determination of HFS and photon radiations from colliding beam. We have taken events with $45 < E - p_z < 65$ GeV and this reduces events with initial state photon radiations and photoproduction events. To have a well defined kinematics the events are selected with $Q^2 > 150$ GeV² and $0.2 < y < 0.7$, where $y \simeq Q^2/xs$ and x is the Bjorken scaling variable.

3 Jet reconstructions

Jets are reconstructed in the lab frame using fastjet anti-kt algorithm with $R = 1.0$ with energy weighted scheme where as inputs HFS objects are taken with $p_T > 0.2$ GeV. The selected jets are with jet $p_T > 5$ GeV within the fiducial region, $-1.5 < \eta < 1.5$, where the pseudo-rapidity variable $\eta = -\ln(\tan(\theta/2))$.

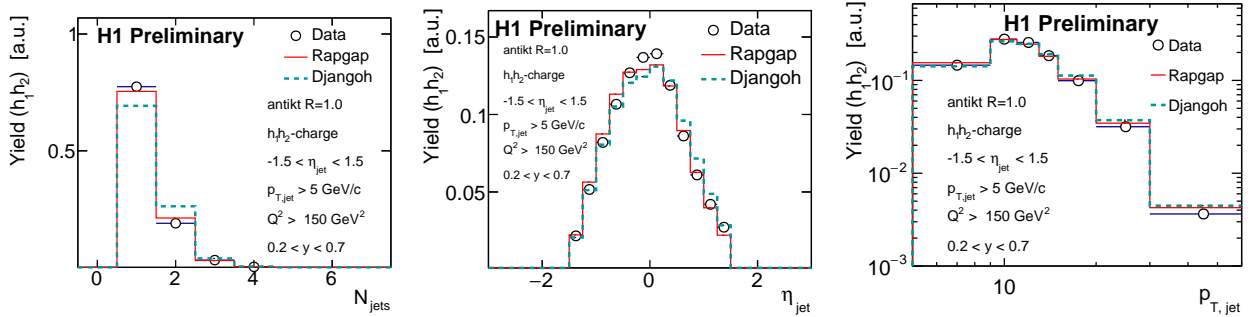


Figure 1: (left) number of jets in an event, (middle) leading jet pseudo-rapidity distributions, (right) leading jet transverse momentum distributions. The jet transverse momentum and pseudorapidity regions are indicated. Only the leading jet is considered for the subsequent analysis, corresponding to more than 90% of all jets. The jet rapidity is restricted in order to match the central tracker acceptance for the jet's leading particle selection. The peak near transverse jet momenta of 10 GeV is a reflection of the $Q^2 > 150$ GeV selection cut.

For the simplicity we are currently using only leading p_T jet which. Two-jet events might be interesting in terms of their origin from higher order processes and in such a case the analysis would be

58 interesting in predicting r_c which might be dominated by jets of gluonic origin. It is to be mentioned
 59 that it requires the leading momentum objects (subjets) within jets to have well defined charge either
 60 $+1$ or -1 . The charge of the subjets are currently picked from the charge of the leading constituents.
 61 Figure 1 shows number of jets, pseudorapidity and transverse momentum distributions. Figure 2
 62 shows some number of constituents in the jet and the momentum sharing for the two leading particles.

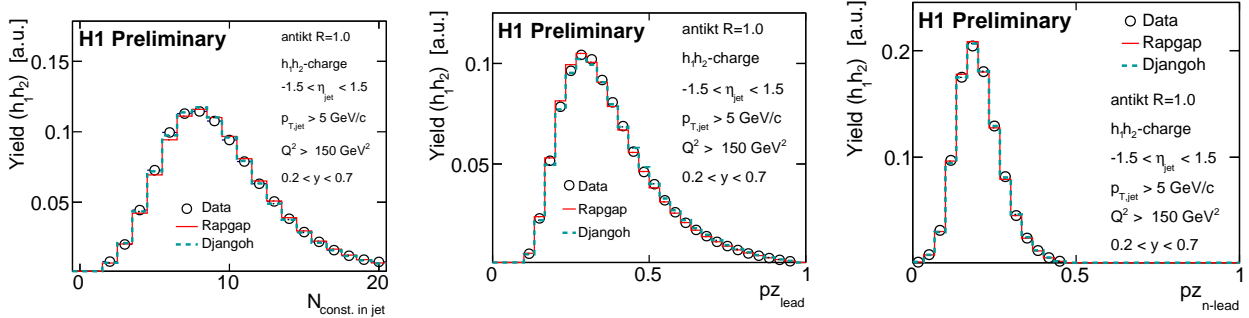


Figure 2: (left) Number of constituents in jets. These contain neutral and charge objects in reconstructed data and MC. Fraction of momentum carried by the leading particle (middle) and next to leading particle (right) along the jet axis.

63 3.1 Recursive soft drop

In the Soft Drop (SD) [5, 6] procedure the constituents of an initial jet with radius R_0 are re-clustered with the Cambridge/Aachen (C/A) algorithm. The soft wide angle emissions are removed that do not satisfy the SD condition. This is a powerful probe of the QCD splitting function. We will use a recursive extension [7] of the SD algorithm, Recursive Soft Drop (RSD), where SD is reapplied along the C/A clustering history until a specified number n of SD conditions are satisfied. The number $n = 1$ corresponds to first split while $n = 2$ would correspond to the second split. The SD conditions we implied is that the leading and next-to leading particles in original jet are found in two separate branches. At the matching we called them as resolved prongs n_R and this senses nonoperative aspects of splitting. Defining z_g and R_g as

$$z_g = \frac{\min(p_{t,1}, p_{t,2})}{p_{t,1} + p_{t,2}} > z_{\text{cut}} \left(\frac{R_g}{R_0} \right)^\beta, \quad (2)$$

$$R_g = \Delta R_{12} = \sqrt{\Delta\eta_{1,2}^2 + \Delta\phi_{1,2}^2}, \quad (3)$$

64 the values for the $\beta = 1$ and $z_{\text{cut}} = 0.2$ is used in the main analysis. $\beta = 1$ means that grooming
 65 using the dynamic radius in reaching successive steps and higher z_{cut} means more harsher cuts on soft
 66 particles.

67 In general it is very informative to see the n_R distributions to check where the correlation of the prongs
 68 and leading particles happens. Specifically z_{cut} has much to do in transforming n_R distributions.
 69 Larger z_{cut} eliminates soft wide angle radiations and the matching probability of the leading hadron
 70 gets enhanced in the first node. Nevertheless, a modest z_{cut} cut would still keep a soft wide angle
 71 component in the first split. The consecutive splits are narrower and thus for the current analysis we
 72 will split the data into 1st prong and 2^{nd+} prongs.

73 **3.1.1 Recursive soft drop: resolved prongs**

74 The kinematics of leading and next-to-leading particles are replaced to that of subjects; i.e, the jet with
 75 $R = 1.0$ is subdivided into smaller jets mimicking the angular ordering of the shower from the final
 76 state particles in jets. Angular order of the branches in the clustering tree is followed through the
 77 hardest branch till the leading hadrons are found in two separate subjects. We call at that point that the
 78 leading next to leading hadrons are get resolved. Soft drop is used with $z_{\text{cut}} = 0.2$ and $\beta = 1$ in order
 79 to remove very soft particles activities surrounding the core hadronization region around the leading
 80 particles. In that way we classify the events with $n_R = 1$ (resolved first prong) and $n_R \geq 2$ (resolved
 81 2nd+ prongs). The first split ($n_R = 1$) is relatively wider angle soft splitting and the 2nd+ ($n_R \geq 2$)
 82 prongs are relatively narrower and harder splitting Figure 3.

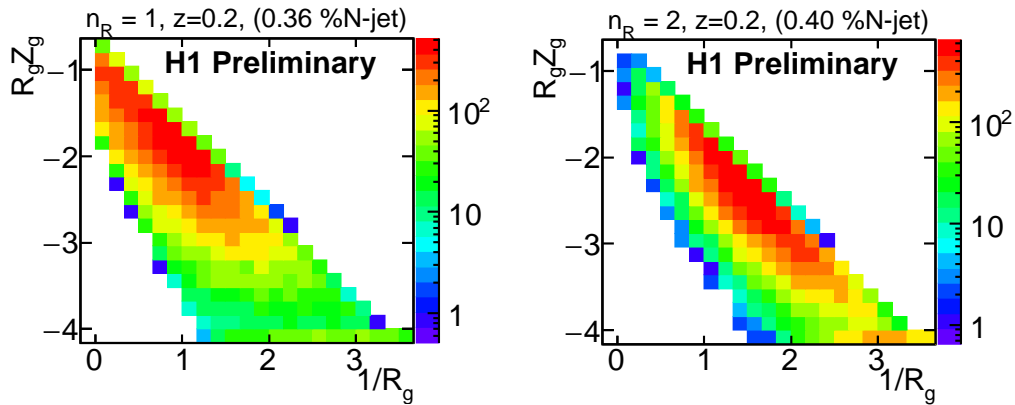


Figure 3: Event distribution in $1/R_g$ vs. $R_g Z_g$ for the first split (left) and for the second split (right).

83 **4 Results: r_c with formation time, k_{\perp} and p_T**

84 Figure 4 shows r_c as a function of t_{form} (left), k_{\perp} (middle) and jet- p_T (right) for different splits and
 85 $h_1 h_2$. The r_c at small formation time (~ 1 fm) is large k_{\perp} or small z origin, and this is the region where
 86 leading and next to leading particles originate from early decorrelations. This region appears to be
 87 purely perturbative in nature. Large formation time (~ 10 fm or more) corresponds to nonperturbative
 88 in nature where $k_{\perp} < 200$ MeV. The striking difference is that at large formation time r_c for the first
 89 split is stronger compared to that of the subsequent splits. Djangoh [3] and Rapgap [4] compare with
 90 data fairly well in most of the region. The systematic bands are the errors appearing from bin-by-bin
 91 corrections using Rapgap and Djangoh event generators. Small k_{\perp} shows strong correlations and this
 92 is the nonperturbative region. Large k_{\perp} appears from wide angle early gluon radiations and this might
 93 trigger independent hadronization which de-correlates the r_c correlations in charge. The r_c for $h_1 h_2$ -
 94 case depends weakly on $p_{T,\text{jet}}$. The first split seems to have stronger dependency with jet transverse
 95 momentum compared to that of the later splits.

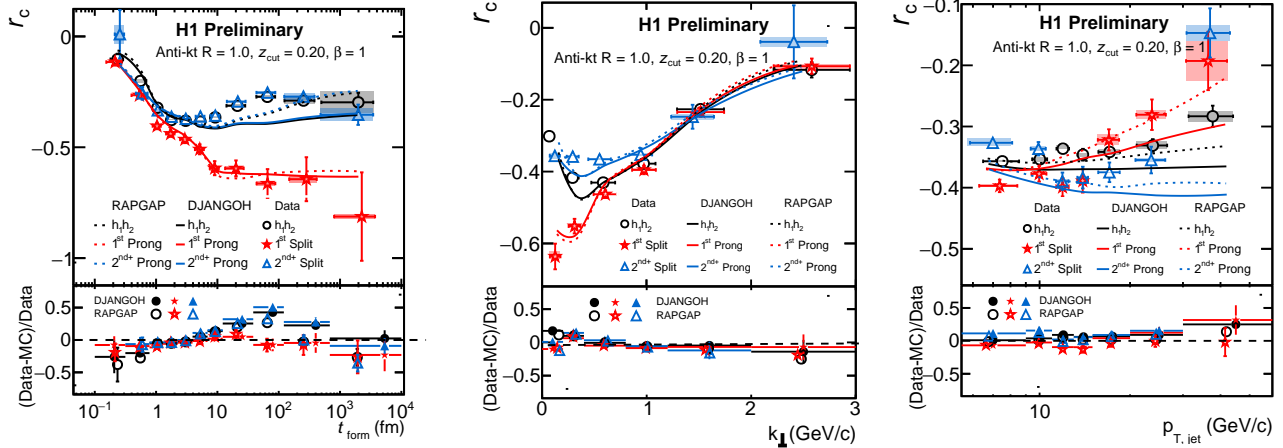


Figure 4: The r_c are shown with (left) formation time, (middle) k_{\perp} and (right) p_T .

5 Summary

The charge correlations r_c is measured at HERA DIS collisions using jets reconstructed using H1 detector. The correlations are negative as expected and the values are compared with Rapgap and Djangoh event generators. The r_c extracted for subjects at first split and later splits shows different values at large formation time. The behavior needs to be studied in details to find out origin of the differences and if this indicates a transition between perturbative and nonperturbative region in formation time scale. Such measurements at H1 in addition to LEP, BELLE, and hadronic pp collisions at the RHIC and the LHC need to be made to understand the dynamics of fragmentation and jet substructure. In particular before EIC these measurements would be very important to understand hadronization and EIC will bring measurement of r_c for different flavor with very high precision.

References

- [1] Y. T. Chien, A. Deshpande, M. M. Mondal and G. Sterman, Phys. Rev. D **105**, no.5, L051502 (2022)
- [2] A. Accardi, Y. T. Chien, D. d'Enterria, A. Deshpande, C. Dilks, P. A. G. Garcia, W. W. Jacobs, F. Krauss, S. L. Gomez and M. M. Mondal, *et al.* [arXiv:2204.02280 [hep-ex]].
- [3] K. Charchula, G. A. Schuler and H. Spiesberger, Comput. Phys. Commun. **81**, 381-402 (1994) doi:10.1016/0010-4655(94)90086-8
- [4] H. Jung, Comput. Phys. Commun. **86**, 147-161 (1995) doi:10.1016/0010-4655(94)00150-Z
- [5] R. Aaij *et al.* [LHCb], JHEP **09**, 006 (2013)
- [6] A. J. Larkoski, S. Marzani, G. Soyez and J. Thaler, JHEP **05**, 146 (2014)
- [7] F. A. Dreyer, L. Necib, G. Soyez and J. Thaler, JHEP **06**, 093 (2018)